

SURFACE POROSITY OF POLISHED GLAZES: EFFECT OF CERTAIN VARIABLES

A. Escardino^(*), J.L. Amorós^(*), M.J. Orts^(*), A. Gozalbo^(*), S. Mestre^(*),
J. Aparisi^(**), F. Ferrando^(**), L. Sánchez^(**)

^(*) Instituto de Tecnología Cerámica (ITC)
Asociación de Investigación de las Industrias Cerámicas
Universitat Jaume I. Castellón. (Spain)

^(**) Esmalglass, S.A.

1. ABSTRACT

At present new aesthetic effects are being sought by polishing the glaze surface. The tiles that are polished can have very thick glaze layers (of the order of 1 mm thickness) produced by dry application of granulars, or finer layers (of the order of 300 μm) applied by the wet method. In the first case, surfaces with specular gloss are achieved, on removing half the original thickness. In the second case, polishing removes between 30 and 50 μm of the glaze layer, providing it with a satin finish. Polishing opens some of the pores occluded in the glaze, converting part of the initially closed porosity into apparent porosity, capable of retaining dirt. Polished surface porosity is determined, amongst other factors, by glaze inner porosity.

The present study addressed the effect, in glazes applied by the wet method, of starting glaze composition and the thermal cycle used in firing on the distribution of resulting glaze inner porosity, and, hence on the apparent porosity found in the polished glaze surface.

2. INTRODUCTION

When a glaze is applied by the wet method, a particle bed forms containing pores that need to be eliminated during firing. Most of the pores that remain in the glaze come from the unfired particle packing^[1]. Initially, the pores are irregular and interconnected, but their size and form varies during the sintering that develops in glassy materials by a viscous flow mechanism^[2,3].

Viscous flow sintering commences at lower temperatures than melting temperatures, concretely at glass softening temperature and, in general, is favoured by increasing temperature, provided crystallisations do not occur^[4]. As the temperature of the system rises, glassy particles soften and liquid phase starts forming. The capillary force of the liquid on the solid particles makes them rearrange to form a more efficient packing, letting the liquid fill (and eliminate) the pores between them. The capillary pressure in the small pores is considerably larger than in the big ones, so that the latter will close later and remain stable during a considerable part of the sintering cycle.

With the rise in temperature, the proportion of liquid phase continues to grow while its viscosity decreases, enabling densification to continue until reaching a maximum, at which not all the pores have been eliminated. A further rise in heat treatment temperature and/or time is detrimental, because it raises trapped gas pressure in the residual pores, increasing pore size and leading to glaze bloating^[5].

If the material is not exclusively glassy, but also contains rigid inclusions inside it, sintering can evolve in a different way. When inclusion volume is less than 10%, densification usually proceeds at the same rate as that of the material free of inclusions. If inclusion volume exceeds 20-30%, it reduces the sintering rate, even halting when the inclusions touch, to form a rigid skeleton that keeps the piece from densifying further^[6,7]. These materials could correspond to ceramic glazes that contain crystalline raw materials, which do not melt during firing, as is the case of zircon or pigments.

If the material that sinters is a devitrifying frit, two processes can develop on exceeding softening temperature: viscous flow sintering, mentioned above, and crystalline phase formation, which usually occurs at the particle surface, hindering particle softening and deformation. When crystallisation takes place before the material reaches maximum densification, sintering can be arrested^[4,8,9].

Ceramic glazes can belong to the three types of materials described previously and the form in which sintering develops can vary, yielding materials with different porosity and different pore sizes.

3. EXPERIMENTAL

Six glazes were prepared with different glassy and crystalline raw materials, in the

proportions detailed in Table 1. A transparent frit (F1), a matt barium frit (F2) and a matt barium and zinc frit (F3) were used as glassy raw materials.

	F1	F2	F3	Kaolin	Quartz	Corundum	Wollastonite	Nepheline
E1	85	--	--	15	--	--	--	--
E2	10	50	20	10	5	5	--	--
E3	--	20	11	6	10	3	5	45
E4	--	85	--	15	--	--	--	--
E5	--	--	85	15	--	--	--	--
E6	31	--	--	6	10	3	5	45

Table 1. Composition (%) of the prepared glazes.

The glazes were wet milled in a laboratory ball mill to a reject of 2 wt% on a 40 μm mesh screen. A fraction of the resulting suspensions was dried and the powder was used to make cylindrical test specimens by pressing, whose shrinkage curve was determined from the evolution of specimen dimensions with temperature using a non-isothermal heat treatment cycle, at a heating rate of 25°C/min, in a hot stage microscope. The shrinkage curve was also determined of each frit used.

To identify the crystalline phases present in the glazes, cylindrical test specimens were prepared by casting the glaze suspensions, and fired at a peak temperature of 1180°C. The fired pieces were milled and analysed by X-ray diffraction (XRD). This test was also run on the test specimens formed with each of the frits making up the glazes.

The glazes were applied by the wet method on green porcelain tile bodies, with different layer thicknesses. Two types of body were used, referenced A and B. After drying, the pieces were fired in an electric laboratory kiln with a floor tile-type thermal cycle (heating rate of 25°C/min to peak temperature with a 6 min hold at this temperature). Test temperatures were 1160, 1180 and 1200°C.

Test specimens measuring 2.5x2.5 cm were cut from the resulting glazed pieces and the thickness of the glaze layer was measured. The test specimen glaze surface was polished in a laboratory polisher, eliminating different layer thicknesses. Polished specimen porosity was determined in an optical microscope connected to an image analysis system, using the clear field signal (direct illumination, in which the pores appear black). Porosity was expressed or quantified as the glaze surface occupied by pores, also determining pore size distribution and mean pore diameter. The glaze surface observed by image analysis in each measurement was 9 mm².

To determine whether pore distribution in the glaze layer was uniform and to relate surface porosity of the polished glaze to porosity in the glaze cross section, glaze cross sections were prepared, embedded in epoxy resin and polished, then determining glaze layer porosity as set out above. In this case, the measured surface was 22 mm², for glazes with a 300 μm layer thickness and 7 mm² for the glazes with a 100-150 μm thickness.

4.RESULTS

4.1. POROSITY OF THE POLISHED GLAZE SURFACE. COMBINED EFFECT OF CERTAIN OPERATING VARIABLES.

Figure 1 plots surface porosity versus layer thickness of glazes E1, E2 and E3 fired at 1160, 1180 and 1200°C, after removing different layer thicknesses.

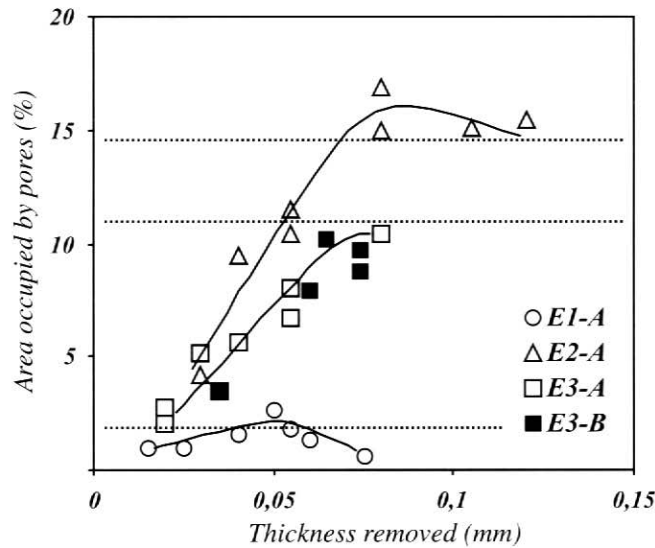


Figure 1. Polished surface porosity vs removed layer thickness of glazes E1, E2 and E3, fired at three temperatures, on bodies A and B.

First of all, porosity is observed to be strongly dependent on the type of glaze. Indeed, at the same removed thickness, E2 is the most porous, followed by E3, while E1 is the least porous glaze.

It should be noted that glaze E2, with the smallest proportion of non-fritted components, is the most porous of the three, implying that the type of frit highly affects end glaze porosity.

The porosity of the polished surface is also observed to depend significantly on removed layer thickness, especially for glazes E2 and E3. This effect is so pronounced that it masks the possible variation in porosity with firing temperature, in the tested temperature range.

In a general way, glaze surface porosity increases with removed thickness, until reaching a maximum approximately corresponding to the removal of 50% of the original glaze thickness.

These results are consistent with the cross section micrographs of these glazes (Figures 2 to 4). Thus, for glazes E2 and E3 which contain large pores (40 to 50µm), glaze layer thickness decreases, pores start surfacing, increasing their apparent radius and

occupied surface until maximising on removal of 50% of the original glaze thickness, as schematically illustrated in Figure 5.

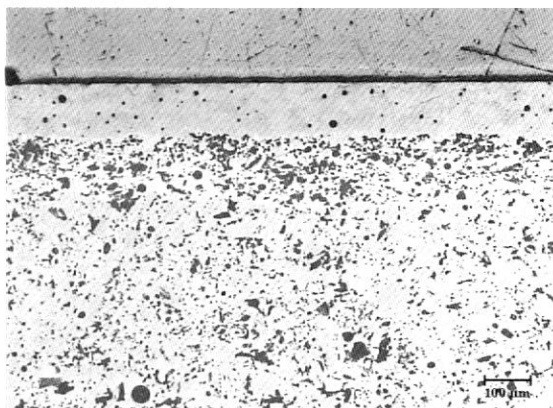


Figure 2. Glaze E1 (1180°C).



Figure 3. Glaze E2 (1180°C).

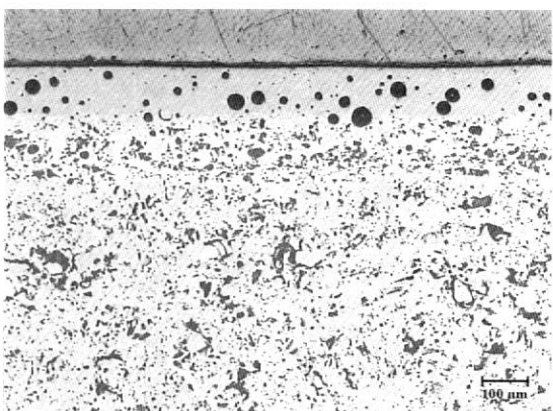


Figure 4. Glaze E3 (1180°C).

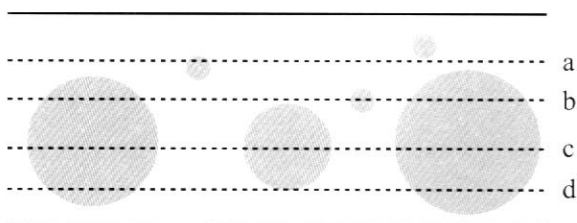


Figure 5. Variation of surface porosity with removed layer thickness.

Glaze E3 was selected to attempt to determine the possible influence of the body on resulting glaze porosity. Figure 1 shows the porosity values for E3 at the three test temperatures and for the two selected porcelain tile bodies. Porosity of the polished surface is observed not to depend on body type. The variation in porosity found in polished industrial pieces, made by applying the same glaze to different bodies, is possibly due to the body's influence on tile curvature, and hence on the thickness of the layer removed in polishing.

Therefore, as the only way of controlling the thickness removed in the industrial polishing operation would be to start with perfectly flat pieces, which ceramic tiles are not, the removed thickness will not be constant in the tile itself or across various tiles, but will vary with tile curvature, causing variations in surface porosity.

4.2. RELATION BETWEEN POLISHED GLAZE SURFACE POROSITY AND POROSITY MEASURED IN THE CROSS SECTION

The results obtained show that to address the study of the effect of the composition on resulting glaze porosity, it is necessary to accurately control the polishing operation. This will only be possible if plots such as those shown in Figure 1 are found for each glaze, and the porosity of different glazes is compared by interpolating the values of their curves, for the same layer thickness removed during polishing. To try and reduce the length of the experimentation, it was attempted to determine if there was any relationship between the porosity of the polished glaze surface and the porosity of the whole glaze layer, measured cross sectionally.

Table 2 details the porosity data of the glazes at 1180°C and mean pore diameter (d_{50}), found by measuring polished cross sections of these glazes. The pore size distributions are presented in Figure 6.

Glaze	ϵ (%)	d_{50} (μm)
E1(1180°C)	1.7	7.5
E2(1180°C)	14.6	24.0
E3(1180°C)	10.9	24.9

Table 2. Porosity of the glazes fired at 1180°C.

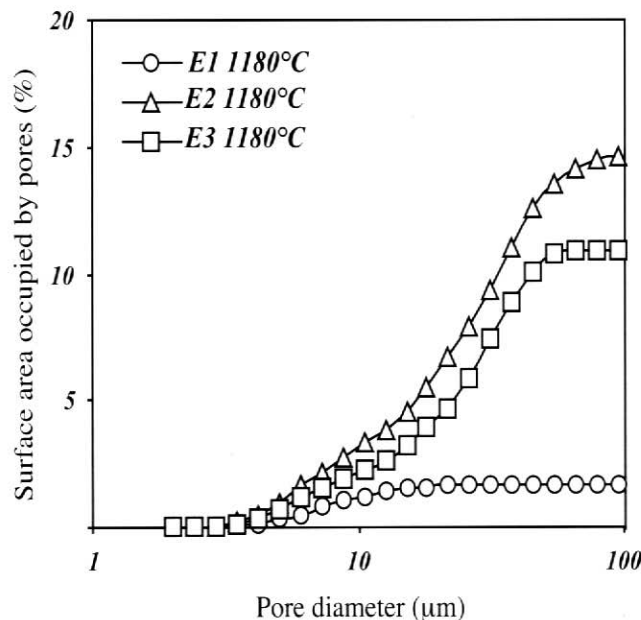


Figure 6. Porosity in cross sections of glazes E1 to E3 fired at 1180°C.

On comparing the surface porosity data of the polished glazes (Figure 1) with the cross sectionally measured porosity values of these same glazes in Table 2 (represented by the dashed lines in Figure 1), the results are found to match. In fact, the value of surface porosity corresponding to half the thickness of the glaze coincides or is lightly larger than the porosity measured in the cross section. The reason is that the porosity in the cross section represents the average for the whole glaze thickness, and next to the surface there are fewer pores and they are smaller than those inside the glaze.

Therefore, to estimate maximum attainable polished surface porosity, it suffices to measure porosity in the glaze cross sections. These cross sections can be prepared for examination (polished) automatically in a laboratory apparatus.

4.3 GLAZE SINTERING

4.3.1 Glaze E1, E2 and E3 shrinkage curves

Most of the pores that remain in a glaze come from the unfired packing^[1], so that it was considered convenient to analyse the elimination of porosity with temperature, by comparing the shrinkage curves of E1, E2 and E3 (Figure 7).

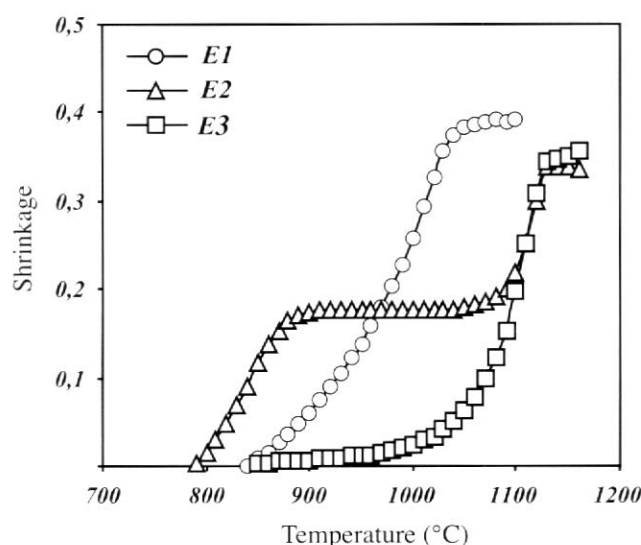


Figure 7. Sintering curves glazes E1 to E3.

The maximum shrinkage of E1 exceeds that of E2 and E3. The three glazes have similar particle size distributions, so that unfired porosity should be very similar. A higher maximum shrinkage value therefore implies that more pores have been eliminated or, in other words, that resulting glaze porosity is smaller, as demonstrated in point 4.1.

Glaze E1 begins to shrink around 840°C and steadily continues to do so on raising temperature until ending at 1080°C. This shrinkage curve is typical of viscous flow sintering, in materials of an exclusively vitreous nature^[4,11].

In glaze E2 sintering starts at 790°C and stops at 890°C, after minor shrinkage (0.18). Test specimen dimensions remain stable up to 1050°C, when densification is reinitiated. This plateau in the shrinkage curve is characteristic of devitrifying materials^[8,11] and is due to the increase in system viscosity owing to crystal formation, which slows down or even stops viscous flow sintering. In two component system, where one is glassy and the other crystalline, in which the glass melts and the crystals do not react during firing, the densification rate has been shown to decrease with the proportion of crystals, ultimately halting when this approaches 30% in volume^[6].

In glaze E3 sintering begins at 840°C and over a wide range of temperatures the shrinkage rate is very low. This could be due to two causes: to a devitrification process, or to the high proportion of crystalline raw materials that it contains [6].

To verify the assumptions made, X-ray diffraction tests were carried out on the glazes produced at 1180°C. The crystalline phases identified in E2 and in E3 were barium orthoclase. Peak intensity was greater in E2, indicating a higher proportion of crystalline phases in this glaze. DTA showed that E2 had an exothermal peak with a maximum at 950°C, and in E3 there was an exothermal peak with a maximum at 850°C, what confirms that, in E2 and E3, crystallisation takes place before reaching maximum densification.

4.3.2. Evolution of glaze porosity with firing temperature

The evolution of glaze porosity was monitored by different techniques, as a function of firing temperature. For temperatures lower than sealing temperature, at which porosity is mainly apparent, this was measured by mercury porosimetry, while at higher temperatures, the glazes were cross-sectionally sliced and their porosity was observed by optical and scanning electron microscopy (SEM).

To study porosity at low temperatures, test specimens were made by pressing from glazes E1, E2 and E3 and fired at cycle peak temperatures of 875, 950 and 1050°C. These firing temperatures were selected because, in this range, both the absolute shrinkage value of the three glazes and the form of the shrinkage curves are very different (Figure 7).

The evolution of porosity and pore size distribution (PSD), measured by mercury porosimetry, are shown in Figures 8 to 10.

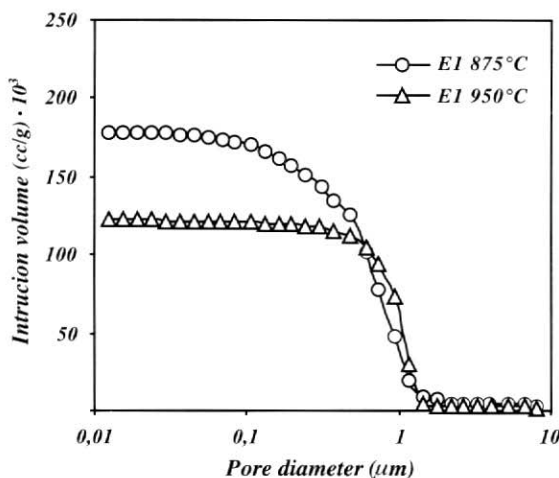


Figure 8. Pore size distribution of E1 at 875 and 950°C.

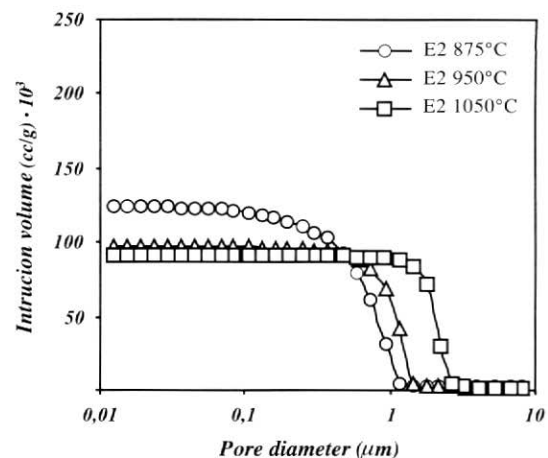


Figure 9. Pore size distribution of E2 fired at 875, 950 and 1050°C.

For glaze E1, a decrease in apparent porosity is observed between 875 and 950°C. The value of apparent porosity is given by the asymptotic value to which each curve tends. At 1050°C there was practically no apparent porosity left, so that the test could not be carried out. These results are consistent with the sintering curve of E1 (Figure 7). It shows that for these glazes, although raising temperature decreases pore volume, their mean pore size (value of the diameter at which the intrusion volume is half the maximum value) hardly changes.

The PSD curves of glaze E2 (Figure 9) also match their shrinkage curve (Figure 7): apparent porosity decreases between 875 and 950°C, and remains constant between 950 and 1050°C. As temperature increases, the curves move toward the right, which means that pore size is increasing, with the largest pores growing at the expense of the smaller ones^[12].

Figure 10 shows that, in the tested temperature range, the porosity of glaze E3 is very high and remains practically constant. However, in this temperature range, although the glaze shrinks very little, pore size grows significantly (the curves move toward the right), just as in the final sintering stages^[11,12].

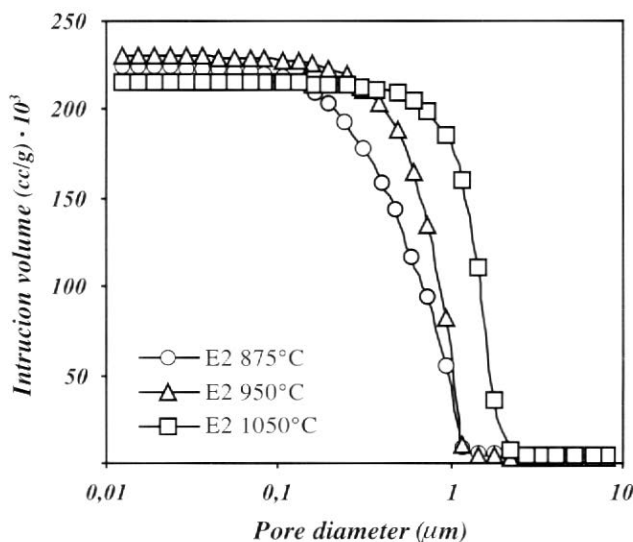


Figure 10. Pore size distribution of E3 fired at 875, 950 and 1050°C.

Figures 11 and 12 correspond to cross sections of bodies to which E2 and E3 had been applied, fired at different peak temperatures, to observe the evolution of applied layer porosity.

It can be noticed that the elimination of porosity commences at the glaze layer surface, because heat transmission is favoured in this area^[3]. In glaze E2 the elimination of open pores seems to have been completed at 1120°C, while in E3 this occurs at 1160°C. At these temperatures, melt effective viscosity is sufficiently low for pores to be spherical. The presence of crystals in the molten mass probably prevents pores from continuing to be removed from these temperatures onwards. For this reason, glaze E1 is the least porous of the three tested glazes. Figures 11 and 12 also show that the surface layer (of approximately 20µm) practically contains no pores, and that polished surface porosity

will vary with removed layer thickness. Moreover, porosity of these glazes is confirmed to hardly alter in the 1160-1180°C temperature range, which agrees with the results of point 4.1, where no variation in polished surface porosity was observed with firing temperature.

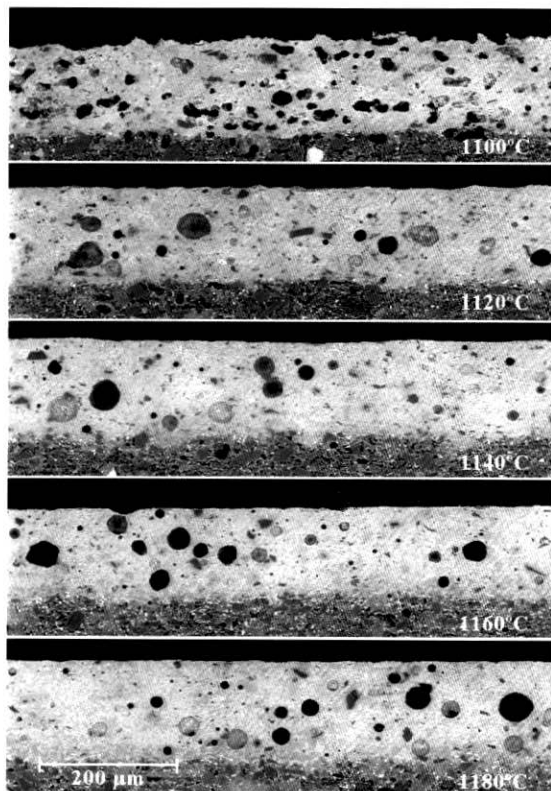


Figure 11. Cross sections of glaze E2, obtained at different temperatures.

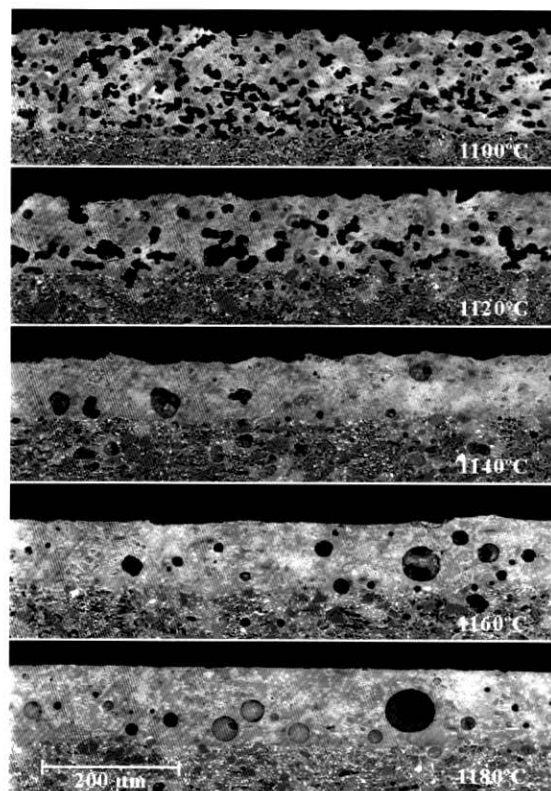


Figure 12. Cross sections of glaze E3, obtained at different temperatures.

4.4. EFFECT OF THE GLAZE COMPOSITION ON RESULTING GLAZE POROSITY

4.4.1 Effect of frit nature

Glazes E4 and E5 were prepared to analyse the effect of frit nature on resulting glaze porosity.

Table 3 details the porosity values and mean pore diameter of the glazes produced by firing at 1180°C. The glaze gloss values found are also included.

Glaze	β (%)	ε (%)	d_{50} (μm)
E1(1180°C)	96	3.2	15.6
E4(1180°C)	12	8.9	16.8
E5(1180°C)	4	8.0	18.9

Table 3. Glazes produced at 1180°C. Glaze layer thickness: 300µm.

The pore size distributions are plotted in Figure 13. The porosity of the glazes containing the matt frit (E4 and E5) is much greater than that of glaze E1. This is because devitrification hinders and even halts pore elimination by viscous flow, since it produces an abrupt increase in the system's effective viscosity^[4,12]. Raising temperature to decrease viscosity is not appropriate, because it leads to pore growth^[12].

Figure 14 plots the glaze sintering curves and Figure 15 presents those corresponding to frits F1, F2 and F3, without any additives.

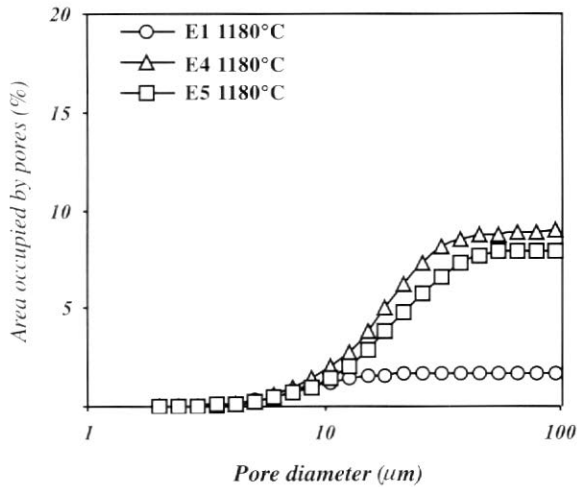


Figure 13. Pore size distribution of glazes E1, E4 and E5, at 1180°C.

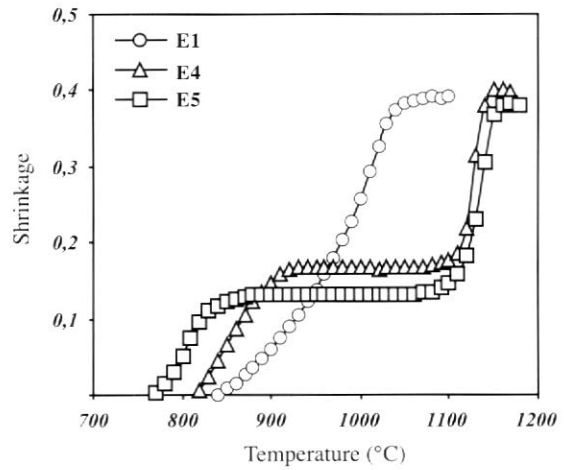


Figure 14. Sintering curves of glazes E1, E4 and E5.

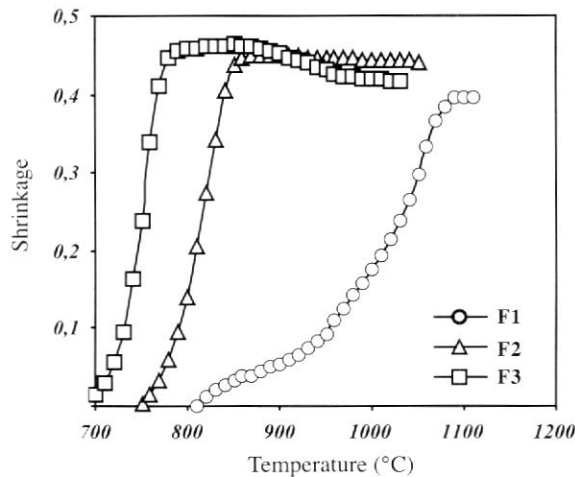


Figure 15. Sintering curves of frits F1, F4 and F5.

It can be inferred from Figure 15 that the most fluxing frit is F3, followed by F2 and F1. Frits F2 and F3 sinter before crystallising, while, surprisingly, frit F1 shows an area where sintering has slowed, which corresponds to cristobalite crystallisation, established by XRD. DTA tests showed that frit F2 began to crystallise at 880°C, and the maximum crystallisation rate occurred at 905°C, while F3 began to crystallise at 800°C, reaching its maximum crystallisation rate at 840°C.

On comparing frit F1, F2 and F3 sintering curves with those of glazes E1, E4 and E5, produced with these frits, the addition of 15 % kaolin is in every case observed to delay sintering onset compared to that of the corresponding frit. This is because at the temperatures at which the test specimen begins to shrink, kaolin behaves as a rigid material. However, the crystallisation process that takes place on the surface of each individual frit particle does not change. In fact, in glaze E4, shrinkage halts at a value of 0.17 at 920°C, and does not restart until exceeding 1100°C. Glaze E5 is much more fluxing (because frit F3 is), and starts sintering earlier; the constant shrinkage segment appears at a lower temperature (850°C) and lasts longer (up to 1090°C).

By analogy with what occurred with E2 and E3, pore growth can be expected to take place in the constant shrinkage segment of E4 and E5, leading at the end of the industrial firing cycle to glazes containing large size pores.

Figures 16 to 18 correspond to the polished cross sections of these glazes. In glaze E1 (1180°C) some dark areas are observed, whose EDS analysis indicates that they are built up of silicon and oxygen, and they should correspond to cristobalite devitrifications. This phase must be found in a very small proportion, since it has not been detected by XRD in the glaze, and sometimes crystallises during sintering of glasses with a high silica content^[14]. In glaze E4 (Figure 17), the barium orthoclase crystals are so numerous that they do not allow seeing the glassy phase in which they are immersed. Glaze E5 (Figure 18) also contains a high quantity of this type of crystals.

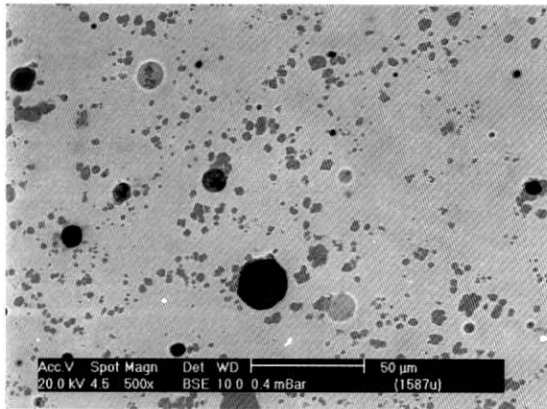


Figure 16. Cross section of glaze E1 (1180°C)

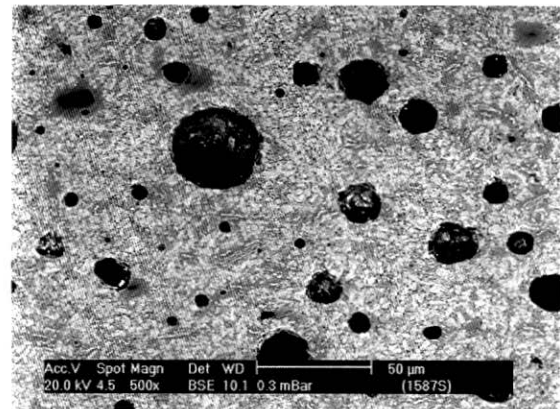


Figure 17. Cross section of glaze E4 (1180°C)

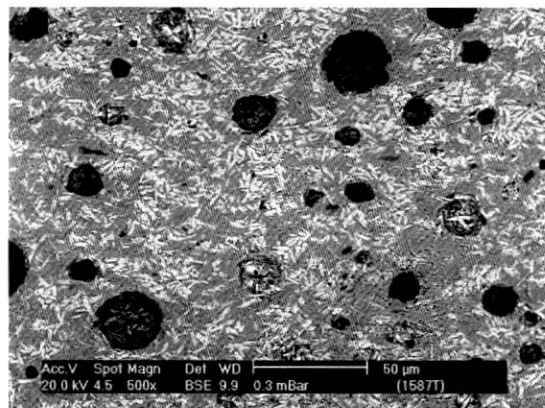


Figure 18. Cross section of glaze E5 (1180°C)

4.4.2 Effect of the introduction of crystalline aggregates in the unfired glaze.

To analyse the influence of the crystalline components of the glaze composition on resulting glaze porosity, glaze E6 was prepared, which had a similar composition to E3, however substituting 20% F2 and 11% F3 by 31% F1. This glaze composition yielded coatings whose porosity was compared with that of glaze E1 and E3. The results, together with the glaze gloss values, are detailed in Table 4.

Glaze	β (%)	ε (%)	d_{50} (μm)
E1(1180°C)	96	3.2	15.6
E3(1180°C)	21	11.0	28.4
E6(1180°C)	90	6.6	23.9

Table 4. Glazes produced at 1180°C. Fired glaze coat thickness: 300 μm .

Comparing the porosity values of E1 and E6 shows that on introducing crystalline components in a glaze consisting of a frit that does not devitrify, or does so to a very minor extent, resulting glaze porosity increases considerably. This is because, as indicated previously, the presence of heterogeneities in the melt hinders sintering^[7]. In fact, the existence of regions in which sintering advances next to others in which it does not, leads to differential shrinkage inside the same test specimen; the areas that shrink most “pull” the others, causing pore size to increase in the latter.

On the other hand, at the same quantity and type of crystalline components in the glaze (glazes E3 and E6), porosity is considerably larger when the glassy raw materials in the glaze are devitrifying frits. These results are consistent with those found in the previous section.

Figure 19 plots the sintering curves of the corresponding glazes. It can be observed that in E6 sintering commences at lower temperatures than in E3, and that glaze E3 maximum shrinkage is smaller, which is consistent with the greater porosity in the resulting glaze.

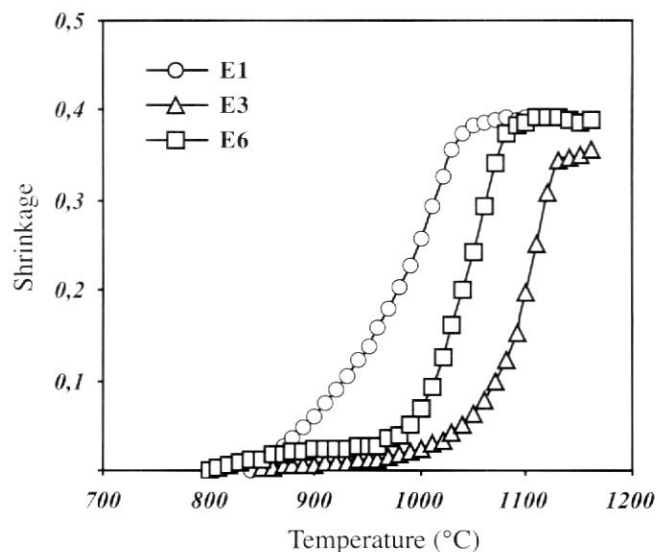


Figure 19. Sintering curves of glazes E1, E3 and E6.

On comparing these curves with each other and observing the sintering curves of the frits (Figure 15), it can be noted that glaze E6, despite the high quantity of crystalline raw materials that it contains, begins to sinter before E1. This could be due to the presence of nepheline, which at the contact points with the frit particles produces eutectic reactions that raise frit meltability. However, the high proportion of rigid material (non-fritted) arrests shrinkage, which does not restart until reaching 970°C.

E3 behaviour is similar to that of E6, but starts sintering later, despite containing frits F2 and F3 which are more fluxing than E1. This indicates that crystallisation in E3 takes place before it starts shrinking, and the constant shrinkage segment represents the influence of the inclusions (which have delayed sintering start) as well as crystallisation (which has impeded its progress).

The appearance of glaze E3 and E6 is shown in Figures 20 and 21. Comparing E6 (Figure 20) with E1 (Figure 16) shows that the former has more glassy phase, indicating that most of the crystalline components in the glaze have dissolved during firing. The fact that more crystals are found in the E1 microstructure and that their porosity is considerably smaller than that of glaze E6 is because cristobalite devitrification in E1 has taken place after sintering, when porosity was already eliminated.

Figure 20 shows the high quantity of crystals found in glaze E3. In fact, the glassy raw materials in this glaze were frits F2 and F3, which are matt. During firing these frits have crystallised, increasing melt viscosity and impeding dissolution of the crystalline raw materials in the glaze. This mixture is the one that has sintered last, and in which resulting glaze porosity is highest.

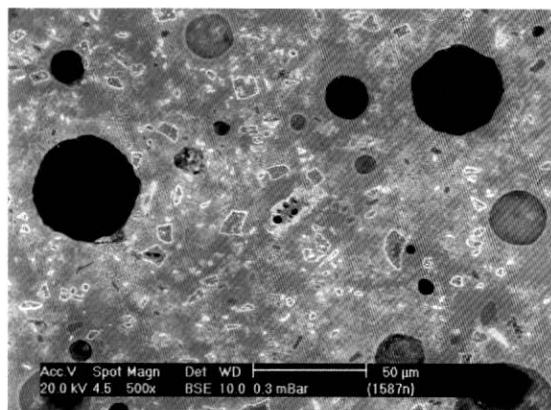


Figure 20. Cross section of glaze E3(1180°C).

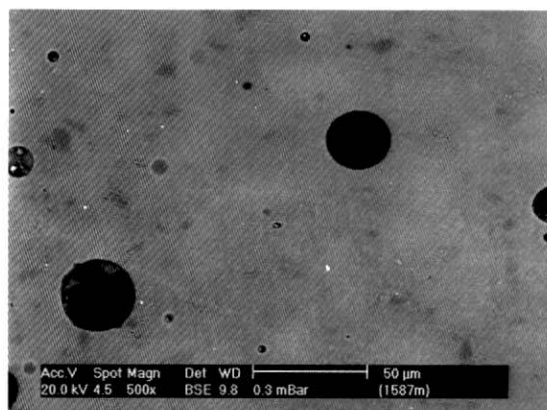


Figure 21. Cross section of glaze E6(1180°C).

5. CONCLUSIONS

In glaze coatings produced by application of glaze suspensions, it has been found that the porosity values obtained on measuring polished cross sections of these glazes are of the order of those found on measuring the polished surface. This last procedure is much more laborious in laboratory-scale tests, so that the former method can be used for porosity studies.

Pore distribution in the glaze layer is not homogeneous. Glaze surface porosity in a polished piece will therefore depend on the thickness of the glaze layer removed during

polishing. Moreover, as the pieces are not flat, removed layer thickness is usually not the same one across the whole piece.

It has been shown that in the tested range, the type of body and thermal cycle do not affect glaze porosity. The influence of these variables, usually observed in industrial tests, is due to the modification of tile curvature and, hence, of the thickness of the layer removed in polishing.

Glaze porosity depends on the starting glaze composition. The lowest porosity is produced when the raw materials are glassy and crystallisations do not occur during the firing. The inclusion of crystalline raw materials in this type of glaze increases resulting glaze porosity.

In a glaze with a high quantity of crystalline raw materials, resulting glaze porosity is higher if the glassy raw materials are frits that devitrify. During firing, crystallisation raises the viscosity of the system and impedes sintering of the glaze layer. On the other hand, if non-devitrifying frits are involved, a melt is produced in which crystalline raw materials dissolve, eliminating pores.

The devitrification of frits F2 and F3 at relatively low temperatures, at which glaze layer porosity has not been eliminated, prevents the advance of densification, and halts pore elimination. The increased viscosity stemming from crystallisation reduces viscous flow sintering. Some authors ^[4,9] use alkaline attack after milling to produce a silica gel layer that hinders surface crystallisation and facilitates pore elimination before this takes place. As a result, the glazes made with devitrifying frits will tend to be more porous than those in which crystals do not form, and in this first group, end porosity will be greater as melt apparent viscosity rises when crystallisation occurs.

When the sintering curves stop, shrinkage does not advance, but the pores continue to grow. When sintering starts again, the abrupt drop in glassy phase viscosity makes the pores close very quickly, preferentially doing so first in the upper part of the glaze surface. This is because surface temperature is higher and it is easier for air to escape and not remain trapped. The pores that remain are large and their size increases further as temperature rises.

6. REFERENCES

- [1] ALVAREZ-ESTRADA, D. Formación y eliminación de burbujas en vidriados cerámicos, *Bol. Soc. Esp. Ceram.*, **1(8)**, 511-525, 1962.
- [2] FERRARIS, M.; VERNÉ, E., Viscous phase sintering of particle-reinforced glass matrix composites, *J. Europ. Ceram. Soc.*, **16**, 421-427, 1996.
- [3] BOCCACCINI, A.R.; ONDRACEK, G. Viscous sintering of non-spherical borosilicate-glass powder, *Glastech. Ber.*, **65(3)**, 73-78, 1992.
- [4] CLARK, T.J.; REED, J.S. Kinetic processes involved in the sintering and crystallization of glass powders, *J. Am. Ceram. Soc.*, **69(11)**, 837-846, 1986.
- [5] ORTS TARI, M.J. *Sinterización de piezas de pavimento gresificado*. Castellón: Universitat de València, Departament d'Enginyeria Química, 1991. [Doctoral dissertation]
- [6] BOCCACCINI, A.R., Sintering of glass matrix composites containing Al₂O₃ platelet inclusions, *J. Mat. Sci.*, **29**, 4273-4278, 1994.
- [7] RAHAMAN, N.M.; De JONGHE, L.C. Effect of rigid inclusions on the sintering of glass powder compacts, *J. Am. Ceram. Soc.*, **70(12)**, C348-C351, 1987.
- [8] ESCARDINO, A. Crystalline glazes. IN: *IV WORLD CONGRESS ON CERAMIC TILE QUALITY*. Castellón: Cámara Oficial de Industria, Comercio y Navegación, 1996. pp. 87-110.
- [9] HELGESSON, C.I. Properties of cordierite glass ceramics produced by sintering and crystallization of glass powder. *Sci. Ceram.*, **8**, 347-61, 1981.
- [10] EPPLER, R.E. Glazing defects and their control, *Ceram. Eng. Sci. Proc.*, **16(3)**, 43-50, 1995.
- [11] AMORÓS, J.L.; ORTS, M.J.; BELDA, A.; GOZALBO, A.; SANMIGUEL, F.; RODRIGO, J.L.; FERRANDO, V. Evolution of glaze porosity in firing. Sintering mechanism and kinetics. IN: *IV WORLD CONGRESS ON CERAMIC TILE QUALITY*. Castellón: Cámara Oficial de Industria, Comercio y Navegación, 1996. pp. 113-132.
- [12] GUTZOV, I.; PASCOVA, R.; KARAMANOV, A.; SCHMELZER, J., The kinetics of surface induced sinter crystallization and the formation of glass-ceramic materials, *J. Mat. Sci.*, **33**, 5265-5273, 1998.
- [13] REIJNEN, P.; FIRATLI, A.C.; GOERG, H.; ARSLAN, R., The mechanisms of pore growth during vitrification, *Cfi/Ber. DKG*, **61(8)**, 441-446, 1984.
- [14] IMANAKA, Y.; AOKI, S.; KAMEHARA, N.; NIWA, K., Cristobalite phase formation in glass/ceramic composites, *J. Am. Ceram. Soc.*, **78(5)**, 1265-1271 (1995).